ONERA

Tiré à Part

Accurate geometrical error model for airborne SAR

H. Cantalloube, C. Nahum

EUROPTO Symposium on Remote Sensing
Florence (Italy), September 20-24, 1999

TP 2000-28

Accurate geometrical error model for airborne SAR

Modèle géométrique d'erreurs précis pour SAR aéroporté

par

H. Cantalloube, C. Nahum

EUROPTO Symposium on Remote Sensing
Florence (Italy), September 20-24, 1999

Résumé : La connaissance précise de la géometrie d'une image SAR aéroporté est vitale pour beaucoup d'applications.
L'interférométrie multi-passe en SAR nécessite une mise en correspondance d'images au dixième de pixel près, alors que d'autres applications telles que la couverture de larges zones par composition d'images ou le géo-référencement sont plus tolérantes et se contentent de mise en correspondance au pixel près.
Comparées au SAR satellitaire, ces exigences sont plus fortes en SAR aéroporté puisque les images ont une résolution plus élevé.
De plus, les irrégularités du mouvement de l'avion dues aux turbulences atmosphériques, introduisent d'importantes distorsions géométriques dans les images.
Malheureusement ces distorsions sont intimement liées au type d'algorithme de traitement de signal utilisé pour synthétiser l'image SAR.
Nous avons développé un modèle géométrique d'erreur adapté à notre processeur SAR hors ligne. Ce modèle fournit une carte des distorsions de l'image.
Les dérivées par rapport aux erreurs sur les paramètres du RADAR ou sur les mesures de la trajectoire de l'avion (vitesse, altitude, oscillations) sont fournies. Elles permettent une estimation efficace des erreurs à partir de mesures de distorsion utilisant des points d'appui.
L'article est illustré par des applications probantes.

(Nb. de pages : 12 ; Fig. : 9)

Ce Tiré à part fait référence au Document d'Accompagnement de Publication DEMR9929

Accurate Geometrical Model for Airborne Synthetic Aperture Radar

Hubert Cantalloube & Carole Nahum
ONERA, Chemin de la Hunière, 91761 PALAISEAU Cedex, France.
Phone: (33) 1 69 93 62 14, Fax: (33) 1 69 93 62 69, email: cantallo@onera.fr

ABSTRACT

The accurate knowledge of the geometry of an airborne SAR image is crucial for many applications:

Repeat-pass SAR interferometry requires an accurate image matching to the 10^{th} of a pixel, while less demanding applications such as wide area coverage by multi-pass composite or image geocoding tolerate mismatches of pixels. Compared to spaceborne SAR, those accuracy requirements are stronger for airborne SAR since they provide higher resolution. Moreover, irregularities in aircraft motion due to air turbulence introduce severe geometrical distortions in the images. Unfortunately, these distortions are tightly coupled with the signal processing algorithm used for computing SAR images.

We have implemented a geometrical error model for our generic off-line SAR processor which provides an image distortion map. Derivatives with respect to errors in radar parameters and errors in aircraft trajectory measurements (velocity, altitude, oscillations) are also provided, thus allowing the efficient estimation of the errors from distortion measurements (tiepoints).
The paper is illustrated with some relevant application examples.

Keywords: Airborne SAR – Geometrical distortion – Image matching – Registration

1. INTRODUCTION

A Synthetic Aperture Radar (SAR) is a coherent radar. That means the sensor emits a light flash (in the radio waveband) and records the phase difference between the emitted flash and its echo back scattered by a target. As any radar (coherent or not), it also evaluates its distance to an object by measuring the time delay between emission and reception. The accuracy of the range estimation depends on the pulse modulation and the receiver sampling rate but is mainly limited by the bandwidth of the electronic amplifier'.

Let us emphasise the significant difference in the order of magnitude of "'range" and phase, which are both estimations of the distance between the antenna and the target. The SAR images which illustrate this paper, have been processed from a signal acquired with a 200 MHz bandwidth. Thus the theoretical range resolution Ar approximates 70 cm according to the formula

$$\Delta r = \frac{c}{2B}$$

where c stands for the light celerity and B the receiver bandwidth.

The radar was set to simultaneously acquire two wavelengths: 10 cm (S-band) or 3cm (X-band). Therefore, a well measurable phase rotation $\Delta\phi$ of, say 36°, corresponds to a range shift δr of 5 mm in S-band and 1.5 mm in X-band. This comes from the propagation equation (accounting for both forth and back propagation)

$$2.\delta r = \frac{\Delta\phi.\lambda}{2\pi}$$

A difficulty arises here since phase measurement is estimated "up to an unknown integer number of turns": Assume that we want to estimate the distance to a target. The range measurement would provide an unambiguous distance estimation with a low accuracy Ar while the phase measurement will provide an estimation accurate to the millimetre, but with an ambiguity of h/2. Since Ar $\gg$ h/2 we are unable to determine which of the ambiguous distances within the range measure mainlobe is the "good one".

Instead of evaluating the distance with an accuracy of one millimetre, the SAR technique classically called "azimuth compression" uses successive phase measurements to resolve the target in the direction of the carrier flight, (designated as "cross-range" or "azimuth" direction). This yields a 2-D image in the rangexazimuth plane.

In order to understand easily this method, let us start with an ideal (though unrealistic) configuration: Assume that during the integration time (portion of antenna trajectory along which the successive echoes are added up), the trajectory remains exactly at the surface of a sphere of radius *R* (it may be a circle but not necessarily so). The received signal is complex-valued, since the radar is coherent and samples both "in phase" and "in quadrature" ($\pi/2$-phase shifted) signals.
Clearly, the echoes backscattered by a target located just at the centre of the sphere add up in modulus, since their phase is constant (the distance between target and antenna is *R)*.

If the target is now slightly moved from the centre along the flight direction (as displayed on Figure 1), then the distance between target and antenna varies slowly during the integration time. Therefore, the phase of the received echoes rotates slowly with time (it is the Doppler effect).

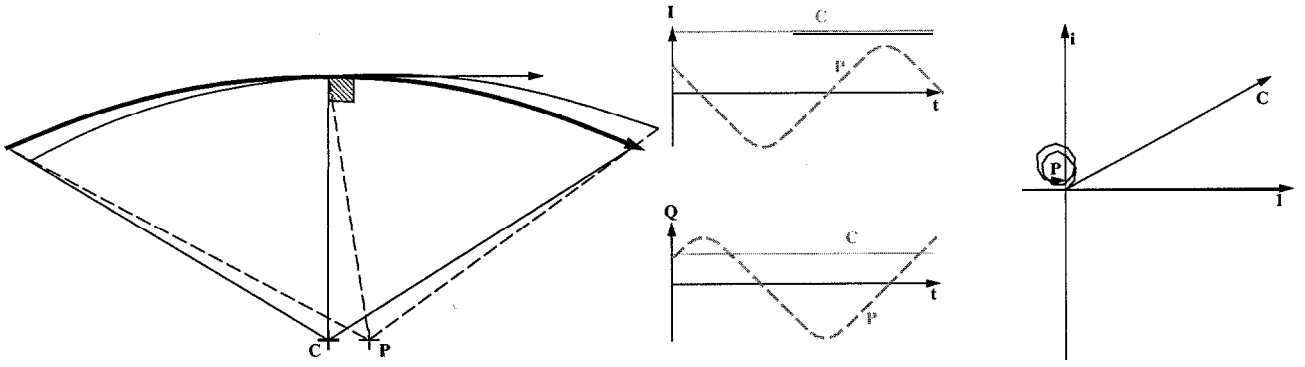

Figure 1 : *perfect case of a trajectory on a sphere centred at C, and P a point separated in azimuth direction (left). Corresponding in phase and in quadrature signals (middle) and their addition in the complex plane (right)*

As a consequence, the corresponding complex values add up to a much smaller modulus (which becomes exactly null if the phase makes an integer number of revolutions during the integration time). The closer the target is from the centre, the slower the phase rotation with time is. Therefore the integration time should be increased in order to improve the azimuth resolution in a SAR image.

Assume now that the target ***P*** is moved along a direction orthogonal to the flight direction. This direction may be either radial (range) or "cross-range and cross-azimuth". The phase rotation is even much slower (at the first order, it is zero because the circle centred at ***P*** is now tangential to the trajectory, only its curvature is wrong) but the above argumentation remains valid:
The depth of focus and the tolerance to elevation shift decreases as integration time increases. The same phenomenon occurs in optics: As the aperture of a reflex camera increases, the depth of focus decreases. In fact, an analogy can be made between the integration time for SAR and the aperture in optics!

In practice, the antenna trajectory does not exactly follow a curve on the surface of a sphere which centres at the target. Moreover, there are many target points, one "target" for each pixel centre of the 2-D computed image. The solution is still to add up the complex signals, but before the addition, the signals should be corrected: Let ***D*** denote the true distance between the antenna and the target. In case ***D*** is different from the sphere radius ***R, we*** will consider the range sample in the echo corresponding to ***D*** and the phase will be rotated by

$$\frac{4\pi(R-D)}{\lambda}$$

This formula is approximative, since the effect of a delay of $2(D-R)/c$ depends on the illumination flash (pulse) modulation technique used. In practice, the pulse can be modulated as a linear ramp of frequency (chirp), eventually demodulated on receive (deramp technique). An alternative is to emit successive pulses with varying frequencies (frequency agility) and combine them in the computer memory into an higher resolution "synthetic pulse". Some radar even combine both techniques (emission of successive chirps with varying middle frequencies). Therefore, the exact formula is very "hardware-dependent" but is not very difficult to deduce from the waveform definition. After that correction, the situation becomes for the target point P similar to the ideal "sphere case".

Traditionally, the above described task is divided into three subtasks respectively called "focusing" (the phase correction corresponding to a perfect linear uniform trajectory), "range migration" (the selection of the sample of range D instead of R) and "motion compensation" (the phase correction corresponding to the difference between the trajectory and the linear uniform "nominal" trajectory). However, in up-to-date SAR-processors those three subtasks (and often even the "range compression" step which performs pulse demodulation) are so interlaced that it is of no use but historical to describe them separately.

2. GEOMETRICAL ERROR MODEL

In the previous section, we (intentionally) dodged a crucial difficulty: the calculation of D, distance between antenna and target to its required accuracy! Retrieving the "target" true location on the ground is not a problem: Depending on the SAR-processor designer choices, a given pixel of the SAR image will be mapped to a given point in some geographic coordinate system. The ground itself may be assumed

'"flat" with height the average flight altitude or a digital elevation model (DEM) may be considered. Therefore, the main difficulty is to estimate the antenna position during the integration time.

The corrected phase should not vary too much to avoid ruining the signal addition. If, for example, the phase should not vary more than 45°, it means (using formula $4\pi(R-D)/\lambda$) that the error on antenna position should be below $\lambda/8$.
In the images illustrating this paper, the integration times are 3 seconds in S-band and 1 s in X-band with an aircraft speed of 80 m/s. This implies that the aircraft position should be estimated with an accuracy of 12.5 mm (*resp.* 3.75 mm) along 240m (*resp.* 80m) trajectory segment (the relative precision approximates *1/20* OOO!) Of course, such a precision on the carrier trajectory is impossible to achieve. However, a global translation error on the trajectory results mostly in a translation of the image with respect to the ground, provided focusing is tuned to a "flat" terrain. If the focusing exploits the DEM, it will obviously be altered since the elevation is incorrect. That is the reason why DEM focusing requires a pre-registration, at least to an accuracy comparable with that of the DEM.

As it will be shown in the last section of this paper, an error on the carrier velocity results, at the first order, in a geometrical distortion of the image. Blurring is in fact a second order effect.

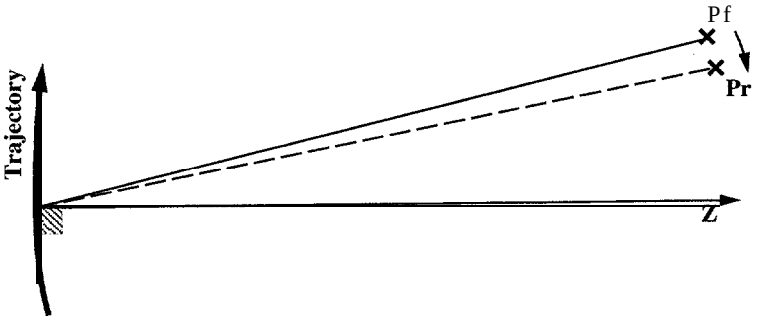

Figure 2: *First order effect of an underestimation of carrier velocity. The phase correction corresponds to a real point P_r closer to the zero-Doppler direction Z than the target point Pfwe are focusing at.*

In order to understand this, assume that we underestimate the aircraft velocity. When we correct the phase for a target point (any pixel centre in the image), we underestimate the phase rotation to compensate, meaning that we compensate for a point closer to the sphere centre than the target point "aimed at". This means that the "effectively compensated" point will appear in the resulting image at the "target" pixel position. In other words, the image will be distorted in such a way that offset between the instantaneous flight direction and the direction of the tangent sphere centre (also called the "zero Doppler" direction since, at first order, distance is constant there) is amplified.

The geometrical effect of any low frequency trajectory error can be derived from this principle: The point effectively focused is the point of the same range to the antenna having the same radial velocity as the aimpoint was assumed to have with the erroneous trajectory during the image synthesis.

Notice that geometrical distortions of a SAR image may also come from errors in the radar parameters themselves. For example, with the ONERA airborne radar RAMSES, unmodelled delays in the demodulation circuits may introduce a bias on the wavelength λ, which would yield the same kind of distortion than a velocity bias. Clock trigger unmodelled delays may also introduce a bias in the range measurements, shifting the whole image along the range axis.

A geometrical error model (GEM) is a routine that establishes the direct coordinate transform rule from a geographical referential to the image coordinates, the inverse coordinate transform rule from the image coordinates to a geographical referential. Those transforms should involve an error parameter vector modelling the low frequencies trajectory errors and some radar parameters errors. In order to increase the numerical efficiency of the routine, the GEM also provides the derivatives of the transforms as well as their partial derivatives with respect to error parameters.

3. AN EXAMPLE OF GEM DESIGN

First of all, in order to create a GEM, one must choose an error parameter vector structure. For the applications illustrating this paper, two radar parameter errors were chosen: a bias on the radar frequency c/λ and a bias on the near range (range of the first echo sample). This

choice was motivated by the waveform type (linear chirp with deramp) and the radar electronics, since those errors can originate from unmodelled time delays in the circuits.

Concerning the trajectory errors, there were used a bias on the initial position (longitude, latitude and altitude), a bias on the heading, a bias on velocity along flight direction, a bias on slope and a set of oscillation terms along the vertical, longitudinal and transversal axes. The number of oscillation terms is "user selectable" depending on the required accuracy of the model. In fact any type of low frequency modelling (such as polynomial, Chebycheff polynomials, Fourier terms...) of the errors could have been used instead.

Once the error parameters structure is established, computer subroutines for direct and inverse coordinate transformations together with their derivatives, must be provided. Here, it was easier to start with inverse transforms:

The designed SAR-processor uses constant squint angle with respect to the nominal trajectory, range also measured with respect to the nominal trajectory, cross-range axis as time and, optionally, DEM elevation data. According to that design, for a pixel of given coordinates in the image, the corresponding focusing point on the ground was computed. With the focusing point coordinate on the ground and the time from the cross-range image coordinate, its nominal range and radial velocity can be calculated, thus its phase rotation speed from the error-free trajectory is deduced. Thereafter the range and phase are modified according to radar parameter error values, in order to obtain effective range and radial velocity.
Using the corrected trajectory, the point on the ground at a given elevation is determined that has this range and radial velocity with respect to the erroneous-trajectory. In fact there are two solutions, one at each side of the aircraft, but only one is on the "imaging side". Thus at this stage, we have designed the procedure (called inverse transform) computing latitude and longitude as a function of the image coordinates, the altitude and the error parameters.

It was relatively easy. by formal derivation of each program line, to get from this procedure another one giving the derivatives of the inverse transform.

The direct transform is slightly more difficult to compute, since given geographical coordinates and an altitude, the erroneous trajectory allows to deduce at each time, range and radial velocity of the point. SAR-processor design choices (and parameters such as the squint angle value of the single-look) allow to find the time (at mid-integration) when the point was focused, by means of a bracketing iteration which is slow. In practice, the iterative search can be initialised from the solution for a close point, thus accelerating considerably the process when we call the function successively for all the pixels of an image.

The formal computation of the derivatives is however not feasible. The solution was to use the image coordinates from the direct transform and invert the Jacobian matrix of the inverse transform in order to obtain the derivative of the direct transform. In a similar manner, the partial derivatives of the direct transform are obtained from the partial derivatives of the inverse transform.

4. SOME RELEVANT APPLICATIONS OF GEM'S

4.1 Multi-look processing

This is certainly the basic application of GEM's. Due to the low directivity of the radar antenna inboard the aircraft, one given point on the ground can be illuminated by the radar during a much longer time than the integration time.
On figure 3A, the point is illuminated from the time it appears under squint 1 (on the forwards side of the antenna lobe) to the time it appears under squint 2 (on the rear side of the antenna lobe). SAR images can be computed for a same point with different integration intervals as represented on figure 3B (on this figure, the two image rows containing the target point for each integration interval, are depicted). Clearly, since the direction of observation is different, the "range axis" in the two images (so called "single-look") do not match (figure 3C).

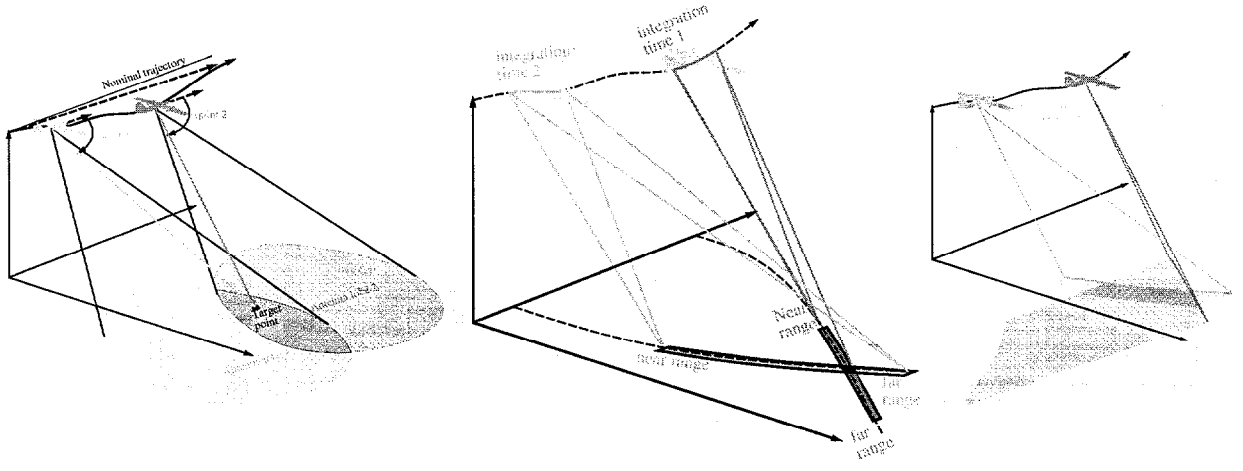

Figure 3: *Principle of multi-look images. The same point on the ground may be imaged from separated integration intervals (synthetic antennae). The corresponding single-look images have their range axis oriented along different squint angles.*

The accurate matching of the single-look images require a good geometrical model, especially if the aircraft trajectory is far from linear (in case the trajectory is linear uniform, a simple skewing maps one single-look to the other).

As it is well known, a multi-look combination has the advantage of reducing the "graininess" (or speckle) of the diffuse reflections on rough surfaces. Thisgraininess is inherent to coherent imaging: holograms obtained by coherent visible light (from a laser) are also "grainy". One of the property of the speckle is that grain locations are independent for single-look images calculated from disjoint integration time intervals, thus averaging several single look images (after co-registration in the same coordinate system) will provide a smoother multi-look image.

This result on "real" rough textures is empirical! In fact, it is related to the statistical characteristics of the texture: Theoretically, a texture with fractal surface (fortunately, unlike any real surface is) would remain grainy whatever the number of looks combined!

Figures 4 and 5 illustrate this application:

The images below illustrate some of the applications described in section 4. The SAR images were obtained from acquisitions of the ONERA airborne SAR RAMSES with linear-chirp deramped-on-receive waveforms in S and X-bands. Images are synthesised with the BID SAR-processor, with flat-terrain hypothesis, Trajectories are estimated by an inertial navigation unit with an error of the order of one nautical mile per hour.

Three single-look images have been calculated with a trajectory hybridisation between GPS and *INU. The GPS correction on the velocity is about IO cm/s. The cut-off frequency (resolution}* is *0.71 m along both range axis and azimuth axis (No windowing). After geocoding, the cut-off frequency along the projection of the range axis becomes 0.82 m. The incidence angle is 60" at mid-swath. Each look has been processed at a constant squint angle. In order to keep an homogeneous azimuth resolution on the whole image, the integration time increases with distance, from 0.71 s at the near range to 0.98 s at the far range end of swath.*

Then the first and the third single-looks have been registered to the middle look geometry and a linear combination of the looks, which optimises the signal to noise ratio, has been computed yielding the smoother 3-look image of Figure 5.

4.2 **Autofocusing**

Some errors in the radar parameters or in the estimated aircraft trajectory, result in mismatches in the single-look images registration, and as a consequence, the multi-look image will be blurred. If the mismatch between the single-looks is measured at several different locations on the image, the GEM will allow to find the error parameter vector that would minimise the resulting mismatch, once integrated to the GEM.

The initial mismatch can be computed by correlating a small patch of one single-look into another single-look. Then the partial derivatives of the coordinate transform rules with respect to the error parameters allow to estimate some values of the error parameters which decrease the mismatch. Reiteration of the process yields an estimation of error parameters that optimises the single-look matching.

This technique called time variant frame drift autofocus ("time variant" means that trajectory correction is not a constant velocity bias, since variations of the mismatch with azimuth are taken into account) is illustrated by the pass at 45" from the runway axis on Figure 7 which was focused with this technique.

4.3 Precise image registration

An other application of GEM'S is to compute precise registered images (PRI). The error parameters are adjusted in order to minimise the distance between ground control points (GCP) and the projection on the ground of their location on the SAR image.
A GCP is a landscape feature of which geographical and altitude coordinates are very accurately known. Once the error parameters are precisely evaluated, the SAR image is projected onto the ground exploiting a DEM of the area, yielding geocoded image of cartographic quality.

On figure 6, the three single-look images of Figure 4 have been matched with a scanned map of the same region assuming that the terrain was flat with an altitude chosen as the mean value given by the radio-altimeter (309 m).
The same single-look images are mapped on Figure 7 using terrain elevation data from NATO's DLMS/DTED *data base. Its planimetric gridding is 62 m x 92 m, its vertical sampling is 1 m, and its altitude values ranges from 250 m to 335 m on the area. One can observe that mismatches remain between map and image, mostly because the DEM smoothes away altitude features thinner than 100 m wide.*

4.4 Aircraft trajectory estimation

As a byproduct of the above error parameters estimation, the determination of the aircraft trajectory can be improved and lead to a better image focusing. This process named single-look to map autofocus, requires however either extremely accurate GCP or a very large number of automatically detected linear features from both map and SAR image because features on paper maps are always displaced to allow printing and reading of the map (if roads were drawn to scale they would be much thinner. And buildings on the sides of roads are always shifted away from the roads !)

4.5 Elevation-dependent motion compensation

Once the trajectory is accurately deduced in 3-D space, it is possible to use the most appropriate terrain elevation model in the focusing. This allows elevation-dependent motion compensation of the SAR-processor.

4.6 Combination of images

PRI from multiple acquisition flights can be combined to create a composite image covering a region larger than the radar swath. The only difficulty is to join without visible seams, portions of images corresponding to different incidence angles. One solution is again to use the GEM for locally calibrating the image to an arbitrary incidence angle. The GEM provides the "viewing direction" from the radar and the DEM gives the local normal to the terrain. With those vectors and the range (or "viewing distance") the local calibration factor can be deduced. This assumes that the surface follows the Lambert's law, which is generally (at least approximatively) the case for extended landscape features. Seamless joints are then generated by using linear combinations between. The weights are calculated in order to minimise the thermal noise of the result, and their sum equals 1.

Figure 7 shows a coverage assembly from three acquisition flights with respective heading 059°, 104° and 149". For each pass, the focusing has been performed by hybridisation GPS-INU except for the pass at 1043 For this image we have used the autofocus technique described above. These images have been registered to the scanned map using ground control points and the DLMS/DTED *DEM.*
For each flight, three looks have been synthesised, hence the common part corresponds to a 9-look image. On purpose, we did not crop away the extreme ranges of the swath (where signal to noise ratio is low and which are contaminated by range ambiguity replicas) for keeping the seams apparent.

4.7 SAR stereogrammetry

When composing SAR images from different acquisition flights, the DEM quality is extremely critical: Any elevation error induces a projection error in the geographical coordinates system, but this error is oriented towards the aircraft trajectory and its magnitude depends on the incidence angle. Therefore, if the viewing angles or headings of overlapping images are different, there is a mismatch in the

super-imposition of the composite image. On the other hand, a measure of this mismatch gives an estimation of the elevation error. This is the principle of the SAR stereogrammetry.

Classically, two SAR images obtained from parallel flight directions thus for two distinct incidence angles are used. But with airborne SAR the flight direction can be changed (unlike the fixed polar orbit plane of satellites such as ERS or RadarSat) one can also compute the elevation of the terrain with SAR multi-heading stereogrammetry.

4.8 Repeat-pass interferometry

In case the trajectories of the different flight acquisitions (on the same area) are too close to deduce a measure of the elevation from super-imposition mismatches, it is still possible to evaluate DEM errors from repeat-pass SAR interferometry. This method exploits the interference pattern between the two images in order to derive the elevation error.

This application is certainly the most demanding in terms of registration accuracy. To understand the reason why, just consider two corresponding pixels in each image of the interferometric pair. Each pixel value corresponds to the sum of ground point contributions around the nominal pixel centre multiplied by a bell-shaped instrumental function (or point-spread function) whose shape and width depend on the radar bandwidth, the integration time and the windowing functions. The "geometrical coherency conditions" on a SAR image pair, allowing it to be used for interferogram generation, is that on the area of the "nominal ground surface" covered by the bell-shaped curve, the optical pathway difference between the two antenna positions shifts the phase difference by a fraction of a turn. A slight misregistration (even below one pixel) reduces dramatically the product of the bell-shaped functions for each image, thus reducing the "meaningfull" part of the interferogram. Since the energy of the interferogram is roughly the same (provided area is homogeneous) the signal to noise ratio drops, hence so does the accuracy of the phase difference estimation which is highly sensitive to noise.

This sub-pixel registration is much more difficult to achieve in the airborne case. The resolution of the images is higher than in the spaceborne case, and the non-linearities in the trajectories make the geometry of the registration non uniform (an accurate GEM is therefore required). The second difficulty comes from the fact that the maximum number of fringes in the interferogram is generally lower. Indeed, one fringe corresponds to a shift of one image with respect to the other of h/2 along the range axis! This shift is not visible at first because the resolution is much lower than h/2. But as the fringes add-up the shift increases to a substantial fraction of a pixel. Since the resolution (width of the bell-shaped curve called "pulse response") is inversely proportional to the radar bandwidth, it is clear that the maximum number of fringes is about twice the inverse of the relative bandwidth (bandwidth divided by the frequency).

This limits the elevation correction from prior knowledge that we can deal with. In practice, the elevation is first evaluated by maximising the coherency between the two images (this is really a coherent version of the SAR-stereogrammetry, but its sensitivity is much higher and it is not ambiguous) and thereafter, the interferogram is computed.

This method is illustrated by Figure 8: We have here used two S-band images along the same path acquired ten days apart. The acquisition flight was done twice because the harsh meteorological conditions (32 knots of wind) ruined the simultaneous acquisition in X-band whose antenna is too directive to accommodate heavy turbulences. The strong back-wind explains why the first image of the pair covers a longer area on the ground though the acquisition duration was the same: the aircraft speed was *increased by 18%.*

The relative bandwidth is 0.07, hence we cannot get more than about 30 fringes (for highest available resolution, the radar can modulate with a relative bandwidth of 0.2 yielding only 10 fringes!). Prior elevation estimation is *done by computing coherency for the elevation of the interpolated* DLMS/DTED *DEM and a set of shifted elevations (by -30 m up to +30 m with 10 m steps) Corresponding interference patterns are printed on the right* side *of Figure 8.*

4.9 Change detection

Mismatches due to elevation errors in composite image super-imposition were mentioned above. But the origin of those mismatches can come from changes in the landscape. This might be the case if the time elapsed between the SAR signal acquisitions is of the order of the hour or the day, or the month. The mismatches may be automatically detected by incoherentchangedetection ("activity detection" or post-strike "damage assessment" for example). But this requires an accurate registration of the images which, since successive flight trajectories could not be exactly identical, requires an accurate GEM.

In case the conditions for repeat-pass SAR interferometry are met, we could also perform a coherent change detection as a byproduct of interferogram generation[3]. Loss of the coherency even if the radiometry remains similar allows to detect that a vehicle or aircraft has been used and parked back (its location has changed at the h-scale though it is not visible at the SAR image resolution). The loss of coherency may also help to decide between growing vegetation and a similar man-made object. It may also signal surface work (ploughing, mine burial...) and sometimes subterraneous activities by the slight vertical motion it causes above it (geosynclinal gas storage or retrieval, nuclear testing...)

Figure 9 shows the incoherent and coherent change detection in the interferometric image pair of Figure 8. Coherency loss areas (appearing as darker spots in the bottom image) are of three kinds: Moved vehicles (dark sharp spots), low backscatter areas (diffuse dark areas as roads and runways or sharp areas as building shadows) and volumetric or wind-sensitive reflectors (forest and the strange rectangular shaped field).
Note that meteorological conditions changed between the acquisitions (rain with 32 knots wind versus calm with a slight snow cover}

4.10 Single-channel MTI

Instead of using SAR images from two separate flights for stereogrammetry or interferometry, one could think of using different looks of the same acquisition. The reason why this strategy would not work is that only non-linearities in the trajectory induce mismatches. To get convinced, just consider that the trajectory is a perfect straight line: The SAR imaging geometrical problem is now axially symmetrical around the trajectory line! Therefore, mismatches are almost negligible in usual situations (this explains why "flat ground" focusing gives acceptable results except in very high resolution cases).

Nevertheless, multi-look mismatch detection has one application: On figure 3B, it is clear that a given target point is imaged under squint angle2 a few seconds after having been imaged under squint angle1. During this time lapse, the object behind the target point might have moved. Thus the comparison of looks may help to perform a kind of Moving Target Indication, the single-channel MTL Of course, there are other more accurate MTI techniques (Adaptive pulse repetition frequency, Space-time adapted processing...) that require multi-channel *i.e.* several antennae separated along the flight direction.

In practice, the locations of moving targets are also erroneous on the single-look images. This is due to the interference of their motion with the image synthesis (which extracts signal according to the radial velocity). However, the GEM can be used to compute the "apparent" positions of a moving target on the different single-look images (simply subtracting the target proper velocity from the aircraft velocity as if it were a "trajectory error")

5. CONCLUSION

Because of the high resolution of the airborne SAR images and the irregularities of the aircraft trajectory which may distort them, a Geometrical Error Model (GEM) must be defined.
The GEM gives the transformation from image position to geographical coordinates together with the inverse transformation and the derivatives with respect to some error parameters.

This paper has been illustrated with some images obtained by the SAR RAMSES designed and operated at ONERA. Among the studied applications of a GEM, multi-look processing, elevation dependent motion compensation, combination of images, repeat-pass interferometry and change detection have been addressed.

BIBLIOGRAPHY

1. Fitch P. Synthetic Aperture Radar Springer-Verlag 1988

2. J.S.Lee A.R. Miller K.W. Hoppel Statistic of phase difference and product magnitude of multi-look processed Gaussian signals Waves in random media 4 1994

3. Corr D.G. Whitehouse SW. Automatic change detection in spaceborne SAR imagery AGARD proc. Toulouse. Oct. 1996.

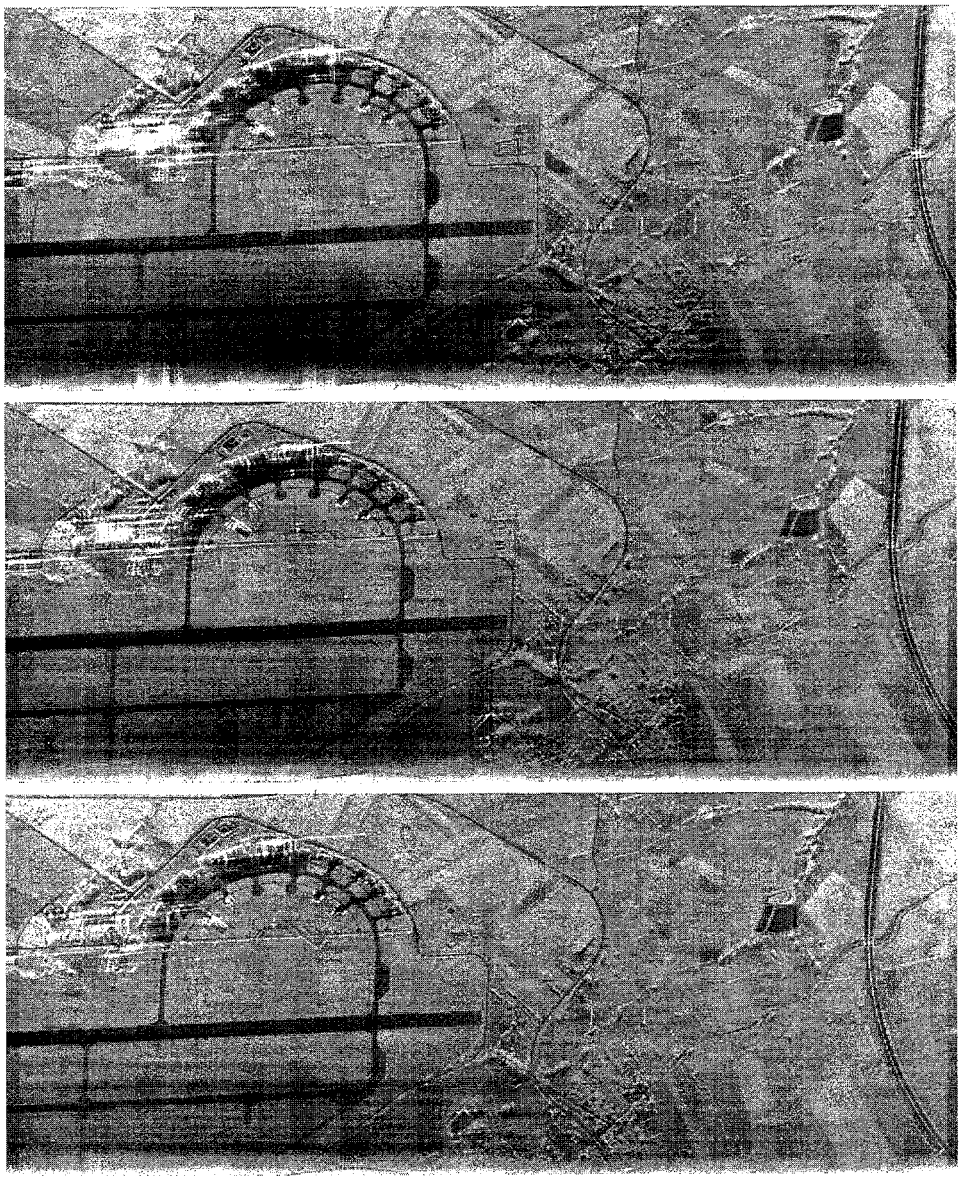

Figure 4: *Three single-look images in X band, squint angle* is *+3.46° (top), +4.77° (middle) and +6.08° (bottom). Geometry is "slant-range" : Range increases to the bottom and azimuth (time) increases to the right.*

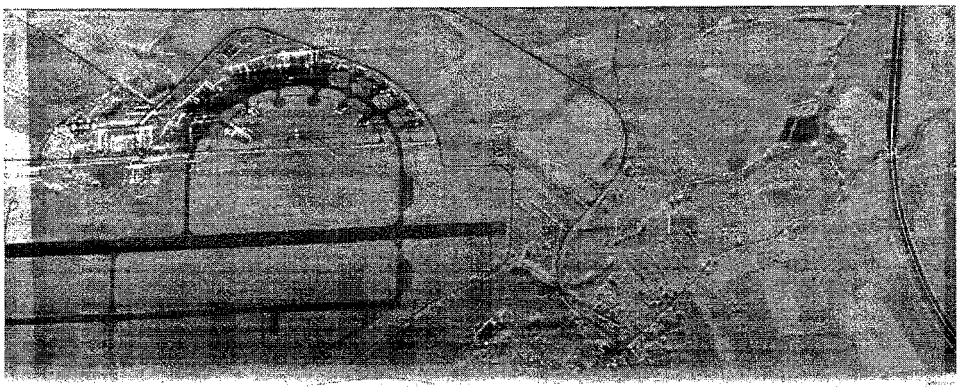

Figure 5: *Three-look composite image from the SLC's of Figure 4. Geometry is that of the middle squint.*

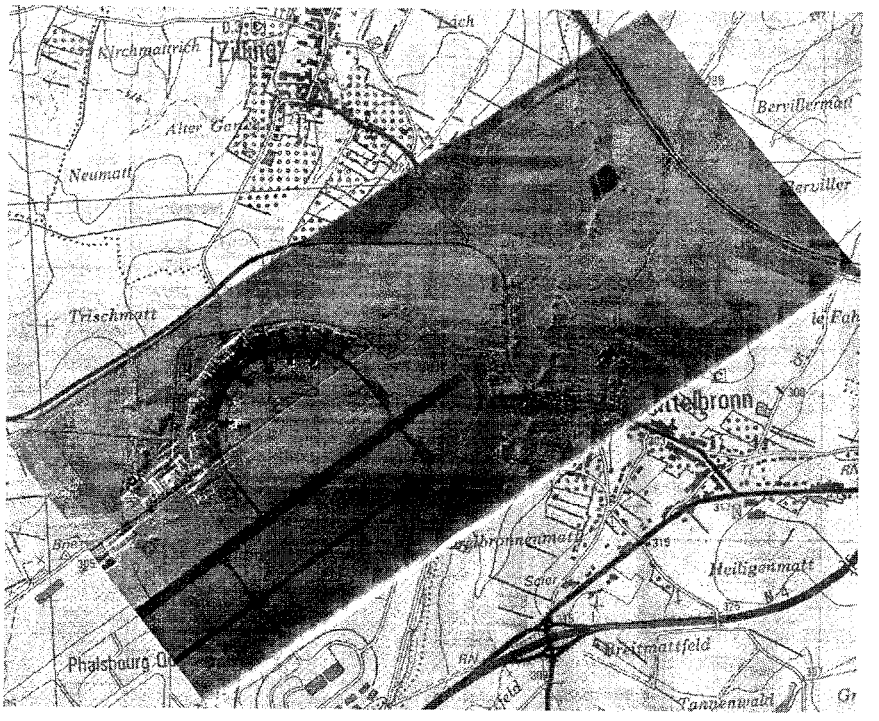

Figure 6 **:** *Projection of the image of figure 5 on a flat terrain.* © *IGN [French National Geographical Institute) for the map background.*

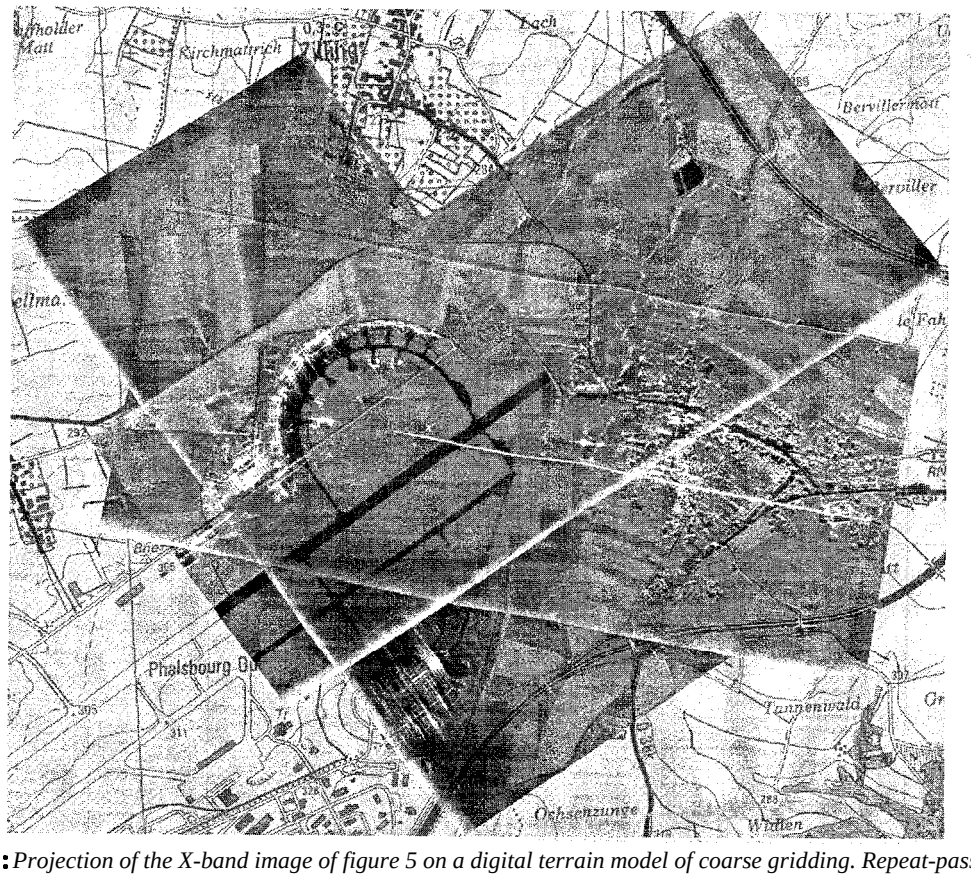

Figure 7 : *Projection of the X-band image of figure 5 on a digital terrain model of coarse gridding. Repeat-pass image composing with two other X-band acquisition.* © *IGN (French National Geographical Institute) for the map background.*

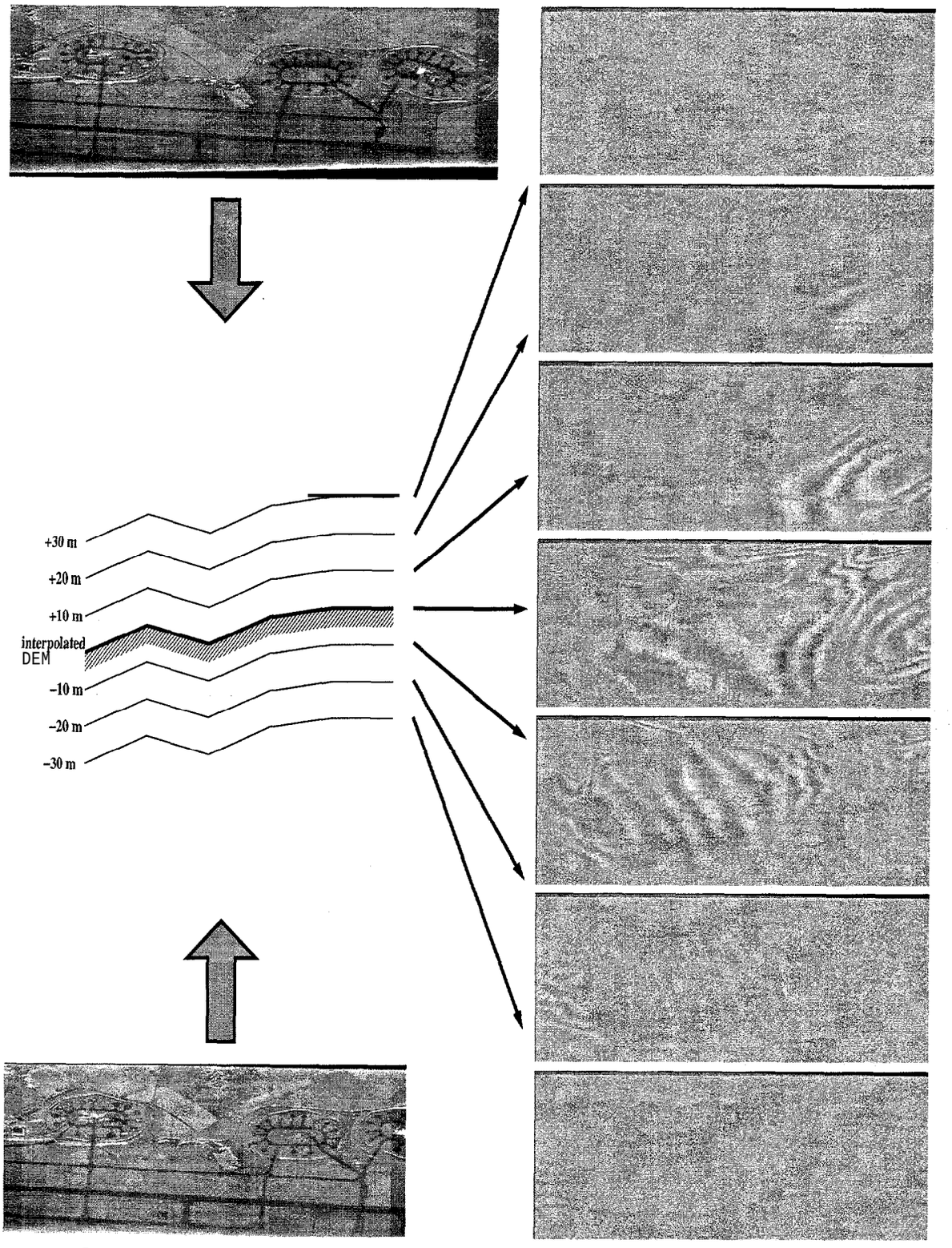

Figure **8:** *Repeat-pass interferograms from two successively acquired S-band images (left). Several interference patterns are computed for surfaces shifted from the interpolated DEM by +30 m down to -30 m (right).*

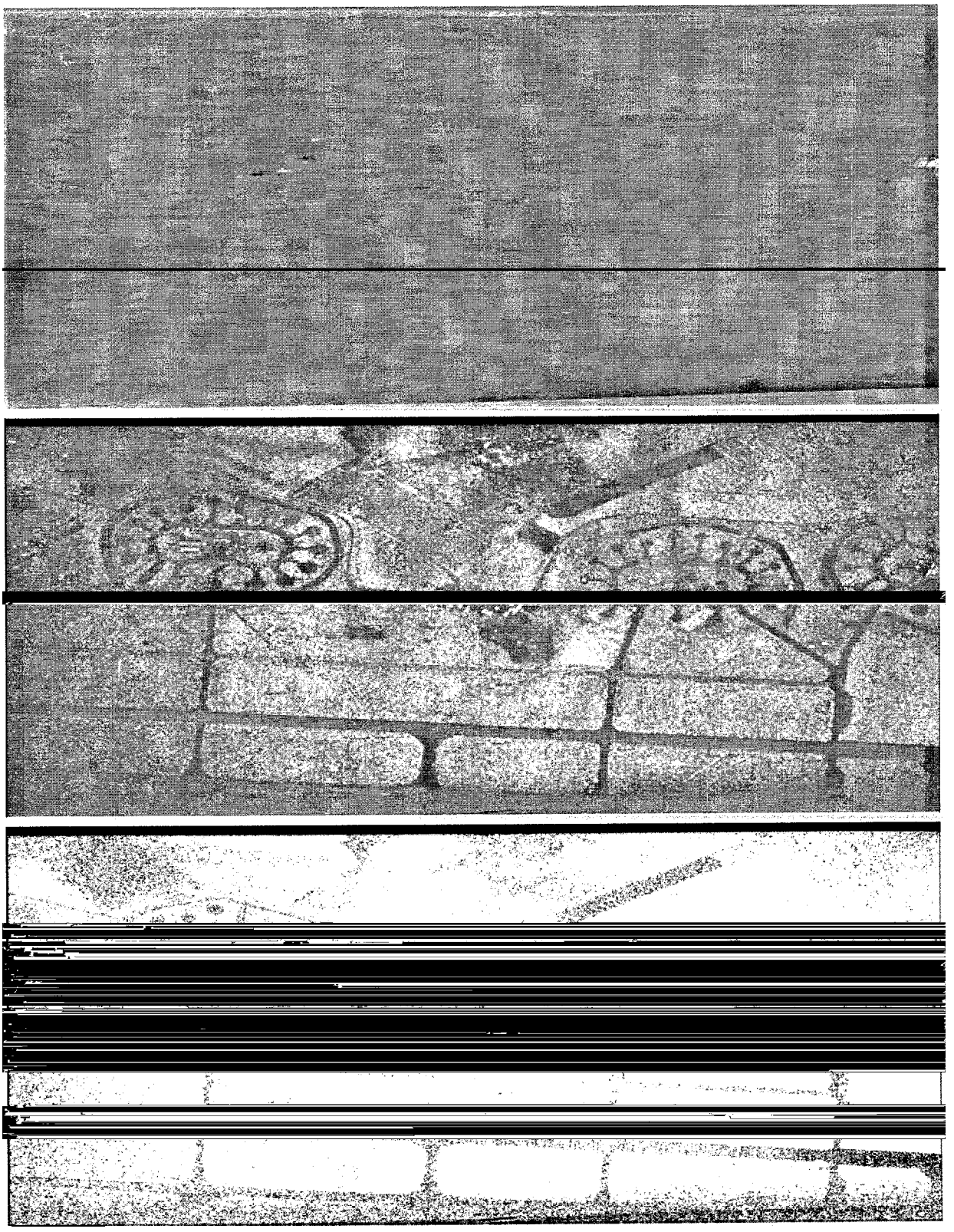

Figure 9 : *Change detection between the images of Figure 8. From top to bottom: Difference image (Reflector disappearances and apparitions are depicted as darker* and *lighter spots respectively), maximum coherency among the elevation-shifted interferograms, and the same image thresholded (coherency losses appear black).*